Quantum Electronics **40** (4) 314–320 (2010)

MEASUREMENT OF LASER RADIATION PARAMETERS

PACS numbers: 42.60.Jf; 07.68.+m
DOI: 10.1070/QE2010v040n04ABEH014202

Extension of the possibilities of a commercial digital camera in detecting spatial intensity distribution of laser radiation

M.V. Konnik, E.A. Manykin, S.N. Starikov

Abstract. **Performance capabilities of commercial digital cameras are demonstrated by the example of a Canon EOS 400D camera in measuring and detecting spatial distributions of laser radiation intensity. It is shown that software extraction of linear data expands the linear dynamic range of the camera by a factor greater than 10, up to 58 dB. Basic measurement characteristics of the camera are obtained in the regime of linear data extraction: the radiometric function, deviation from linearity, dynamic range, temporal and spatial noises (both dark and those depending on the signal value). The parameters obtained correspond to those of technical measuring cameras.**

Keywords: *commercial digital camera, spatial distribution of radiation intensity, software extraction of linear data, dynamic range, temporal and spatial noise.*

1. Introduction

In modern commercial digital cameras high-quality solid-state photosensitive arrays are used. One may use such inexpensive commercial cameras as a detector instead of technical cameras in various practical applications. For example, such applications may be microscopic systems [1], industrial displays [2], and hybrid optical-digital recognition systems [3, 4].

The main problem in using digital cameras as measuring devices is that the electronic system of the camera performs processing of the detected image in order to convert it to an image file. In saving the detected image in various formats of processed data (for example, JPG or TIF) the dynamic range and linearity of the signal are irreversibly corrupted, which limits the possibilities of such digital cameras in experimental techniques. This is more pronounced in detecting laser radiation, which is characterised by a large dynamic range.

Nevertheless, modern single-lens reflex (SLR) cameras are capable of saving images in an unprocessed raw format. By using the methods of extracting linear data, which include special software raw-converters, one may obtain linear unprocessed images from commercial digital cameras, both for detecting and measuring the spatial distributions of laser radiation intensities with large dynamic range.

Among special software raw-converters it worth noting the program dcraw with an open source code [5]. This converter was used for estimating the characteristics of digital cameras [6] and in the optical-digital display system [7]. Note that the dcraw converter can be used for processing raw-files of more than 400 types of commercial digital cameras.

The present work is aimed at demonstrating potential possibilities of commercial cameras in measuring the spatial distributions of laser radiation intensity and at estimating the measuring capabilities of the cameras. The Canon EOS 400D digital SLR camera was chosen as an example. The camera signal linearity was experimentally demonstrated by the example of detecting the far-field diffraction on a rectangular hole. The experimental data are compared with numerical simulation. For this camera, the radiometric function was measured and the linear and full dynamic ranges were determined. The temporal and spatial dark noise and noise dependent on the value of detected signal are presented.

2. Linear data extraction from commercial camera

In this section we describe the procedure for extracting linear data by the example of color camera Canon EOS 400D with a 12-bit ADC.

In detecting spatial distributions of light intensity by commercial cameras the latter should operate in the raw-format regime. In this case the image will be saved in the unprocessed format with the extension cr2 (the extension may differ for other cameras). This item is important because JPG and TIF formats inevitably lose a part of the dynamic range and linearity of the detected signal.

After saving the image in the raw-format the dcraw-converter should be employed in the so-called 'document' regime for obtaining the linear data. This is made by running command *dcraw -4 –T –D filename.cr2*, where *filename.cr2* is the name of the raw-file with the detected image. The linear 12-bit data obtained in this way from the raw-file with the name *filename.cr2* will be saved in a 16-bit TIF file with the name *filename.tif*.

M.V. Konnik, S.N. Starikov National Research Nuclear University "MEPhI", Kashirskoe sh. 31, 115409 Moscow, Russia;
e-mail: holo@pico.mephi.ru;
E.A. Manykin Russian Research Center "Kurchatov Institute", pl. Akad. Kurchatova 1, 123182 Moscow, Russia;
e-mail: edmany@isssph.kiae.ru

Received 5 August 2009; revision received 10 February 2010
Kvantovaya Elektronika **40** (4) 314–320 (2010)
Translated by N.A. Raspopov

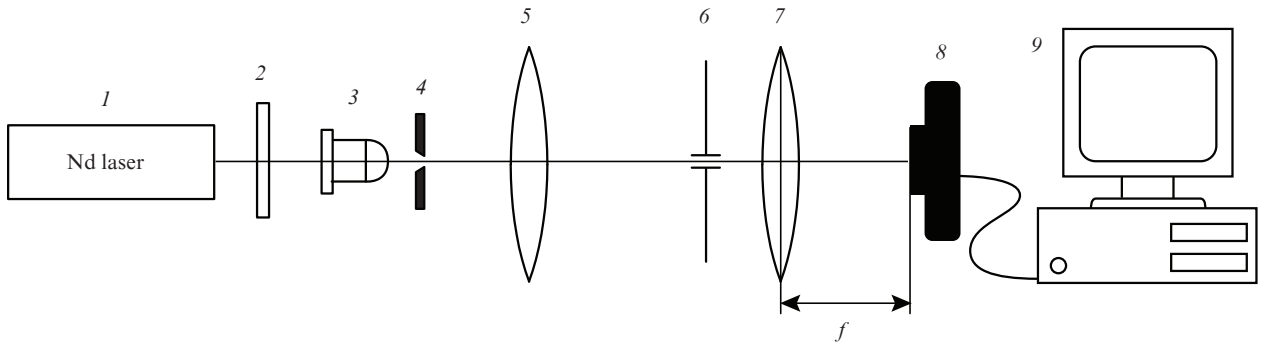

Figure 1. Scheme for detecting diffraction pattern: (*1*) neodymium laser; (*2*) attenuator filter; (*3*) microscopic objective; (*4*) spatial frequency filter; (*5*, *7*) objectives; (*6*) diaphragm; (*8*) digital camera; (*9*) computer.

In the linearised image file, the signal value is proportional to the detected light signal. The image itself is half-tone one and repeats the RGGB-structure of the Bayer color filter array [8]. This means that each pixel comprises information on the value of the light flux passed through the corresponding color filter. From the image obtained one should select three images corresponding to different filters: red, blue (1/4 of all pixels each), and green (1/2 of all pixels) by software means. For example, the image detected in the monochromatic light of He–Ne laser may be obtained by selecting pixels in the odd rows and columns of the unprocessed linearised image. It is convenient to view and analyse such images by the graphical analyser NIP2 [9, 10]. In the opposite case, rescaling of 12-bit image signals to 16 bits is needed for viewing in ordinary graphical editors.

In the following analysis of measured laser intensity distributions with narrow spectrum it is appropriate to use one of the images corresponding to the most transmitting filter for the radiation under study. In addition, if necessary two other images can be used for obtaining measuring images with the dynamic range exceeding the dynamic range of photosensitive array [11].

The linear measuring images comprise data that can be used for evaluating the commercial camera as a measuring device (estimating the dark and signal noise, dynamic range, and presence of periodical defects in the photosensitive array).

3. Experimental demonstration of camera signal linearity

To demonstrate the linear response of commercial camera to light signal we detected the far-field diffraction pattern from a rectangular hole.

The experimental setup is schematically shown in Fig. 1. Second harmonics of a neodimium laser with the wavelength $\lambda = 0.53$ μm (obtained with KDP crystal) is attenuated by filter (*2*) and focused by microscope objective (*3*) to the spatial frequency filter (*4*). The radiation collimated by objective (*5*) passes to the rectangular diaphragm (*6*) (with the aperture $l_x = 130$ μm and $l_y = 200$ μm). The far-field diffraction pattern formed in the back focal plane of objective (*7*) ($f = 500$ mm) is detected by the photosensor of commercial camera (*8*) (with the camera objective removed) and saved in the raw-format for further processing and analysis. The camera has color CMOS photosensor with the Bayer filter array (3888×2592 pixels with the pixel size of 5.7×5.7 μm) and a 12-bit ADC. Computer (*9*) controls digital camera (*8*) and processes the detected images.

Intensity I of light diffracting on the rectangular diaphragm in the back focal objective plane is given by the relationship [12]

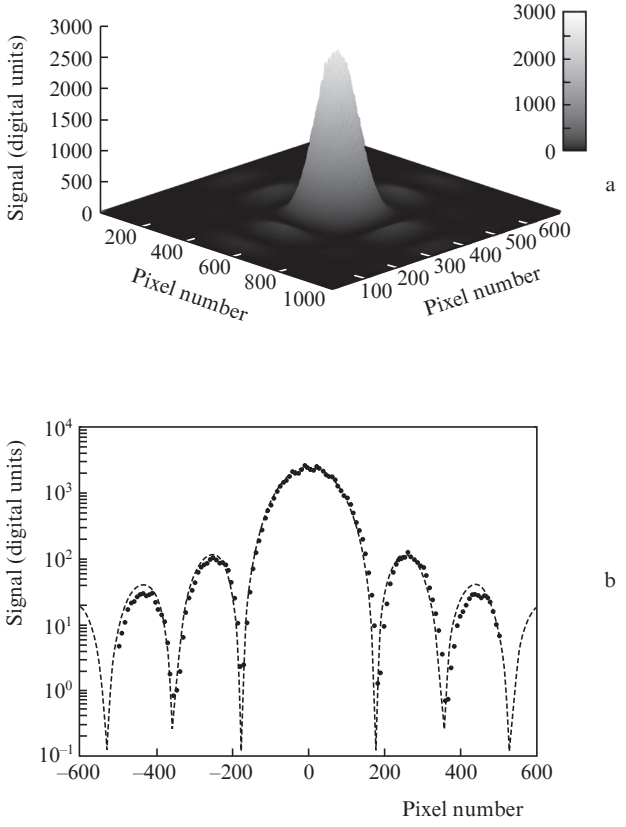

Figure 2. Experimental results of detecting the diffraction pattern from rectangular hole: (a) spatial intensity distribution; (b) comparison of experimental data (points) with calculated (dotted curve) for the central horizontal cross-section.

$$I(x_0, y_0) = I_0\left(\frac{\sin k_1}{k_1}\right)^2\left(\frac{\sin k_2}{k_2}\right)^2, \quad (1)$$

where $k_1 = l_x x_0/(\lambda f)$; $k_2 = l_y y_0/(\lambda f)$; x_0 and y_0 are the coordinates in the sensor plane. According to (1) the zero diffraction maximum width $\Delta x_0 = 2\lambda f/l_x$ in this case is 4.0 mm.

The diffraction pattern detected by the camera was then processed by the dcraw-converter in the 'document' regime (the half-tone completely unprocessed image without interpolation). Two green color channels corresponding to the laser illumination were selected from the 'raw' data array processed by the dcraw-converter, the black level offset (256 digital units) was subtracted, and the data were averaged. This procedure provides obtaining the linear image for measuring purposes (see Fig. 2a).

Then the width of zero diffraction maximum was measured and the number of occupied pixels was calculated. The zero maximum width of the diffraction pattern detected by the photosensitive array was 352 pixels. Since the period of pixel disposition in each color channel is 11.4 μm, the width of diffraction order is 4.1±0.1 mm, which agrees with the results calculated by formula (1).

Comparison of the detected and calculated intensity distributions for the central horizontal cross-section of the image is shown in Fig. 2b. The experimental data were approximated to the theoretical function by using the least square method. One can see that the detected intensity distribution is close to the theoretical function (the LSQ error of approximation is about 1.7%).

Thus, we may conclude that the camera response to light is linear. Hence, the commercial digital camera can be employed in the mentioned regime of data processing as a measuring device.

4. Estimation of camera measuring characteristics

Consider the measuring characteristics of the commercial camera: the dependence of signal value on exposure (the radiometric function), black level offset (BLO), temporal dark noise, spatial dark noise, temporal noise dependent on the signal, spatial nonuniformity of the photo response, and linear and full dynamic ranges. White light emitting diodes were chosen as the source of illumination. The results are presented for the green color channel only because in the other channels they coincide within the accuracy of measurements. The measurements were taken according to the PixeLink instructions [13] and to EMVA1288 standard [14]. The procedures for estimating the measuring capabilities of camera based on the requirements of mentioned documents are realised as programs in the mathematical calculation language MATLAB.

4.1. Camera response linearity

The radiometric function of the camera was measured by detecting images of a plane light field at various exposures. Illumination light inhomogeneity was eliminated by using a matrix of white LEDs and a scattering glass plate. The exposure time for the detected images varied from 1/4000 to 10 s. The sensitivity of the camera was set to minimum (ISO 100). Four images were taken and averaged for each particular exposure, and the standard deviation was taken as the measurement error. The frame central domain of 64×64 pixels from the averaged image was used for analysing the statistical parameters of the detected light signal. The detected images of the plane field were first processed by the authorised converter supplied with the camera. The images were saved in the 16-bit TIF format (the BLO value was subtracted automatically). One can see from Fig. 3 that the radiometric function obtained is not linear, which is caused by the post-processing procedures automatically performed by the camera such as gamma-correction, color interpolation, and enhancement of visual quality. The radiometric function can only be accepted as linear in a small exposure range (see Fig. 3b).

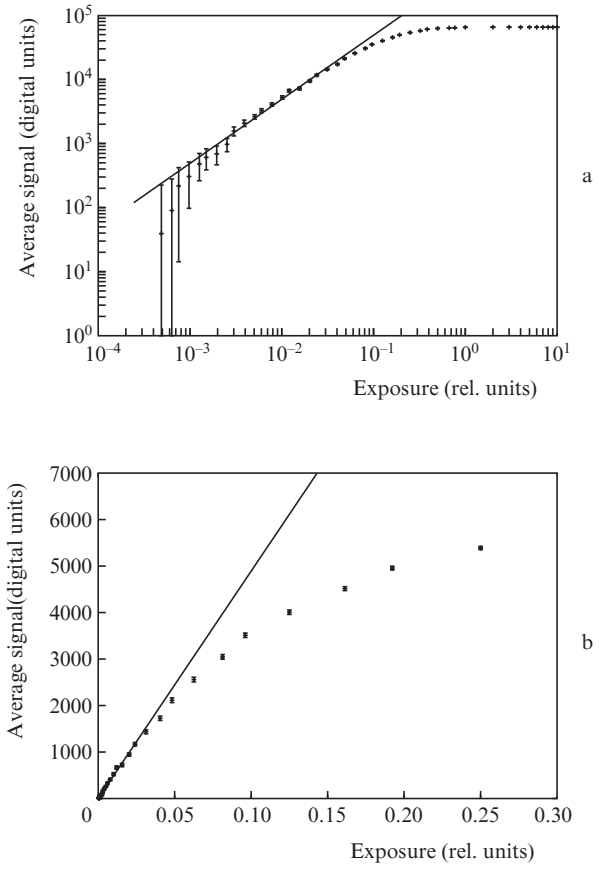

Figure 3. Radiometric function obtained by using authorised software converter for image processing. Average signal amplitude versus the relative exposure at small (a) and high (b) values. Solid curve is the approximating linear function.

Then the data were processed by the special dcraw-converter in the 'document' regime without interpolation and gamma-correction. The detected images were converted by this converter to 12-bit 'raw' data and saved in the 16-bit TIF format (the BLO magnitude equal to 256 digital units was subtracted). As is seen in Fig. 4, the obtained signal is linear up to 3470 digital units, i.e. the beginning of the photosensor saturation region. The errors presented in Fig. 4 correspond to the standard deviation from the average signal.

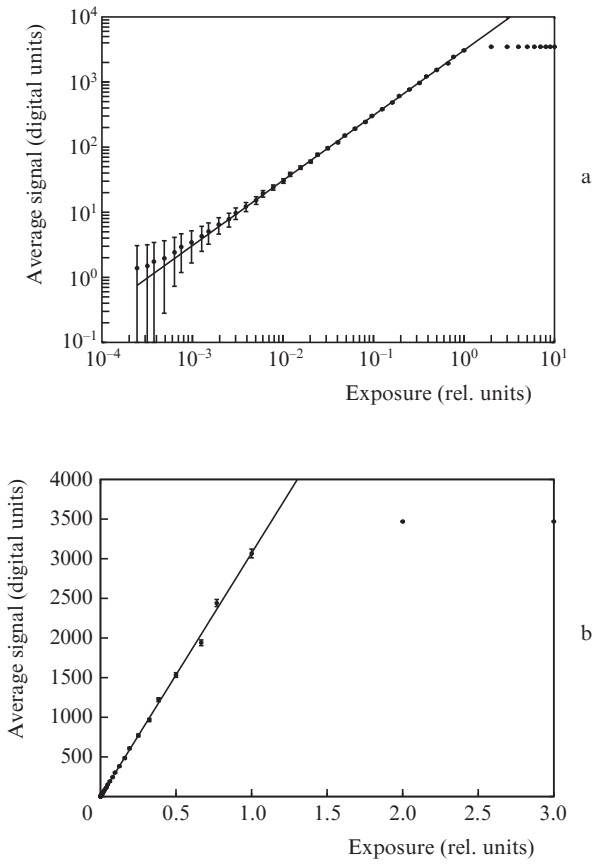

Figure 4. Radiometric function obtained by using dcraw-converter for image processing. Average signal amplitude versus the relative exposure at small (a) and high (b) values. Solid curve is the approximating linear function.

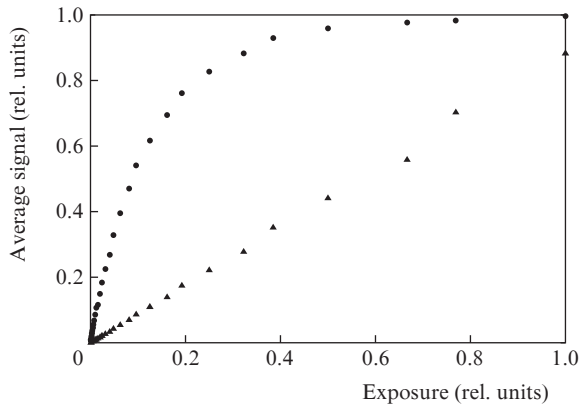

Figure 5. Normalised radiometric functions obtained by using authorised converter (dots) and by dcraw-converter (triangles).

Comparison of the radiometric functions in Fig. 4 and Fig. 3 shows that the dcraw-converter provides the linear detected signal in a noticeably wider range of exposures (see Fig. 5). Quantitative estimates of the linear dynamic range in the cases of the authorised program converter and the dcraw-converter are given in Section 4.4.

For the radiometric function obtained with the dcraw-converter (see Fig. 4) we estimated the maximal deviation from linearity. According to the EMVA1288 standard [14] this deviation (percent) from the saturated signal for signal magnitudes μ within the range 5%–95% is given by the expression

$$L_E = \frac{C_m^{\max} - C_m^{\min}}{2}. \tag{2}$$

The deviations C_m are estimated for each mth measuring point of radiometric function by comparing with the regression line

$$C_m = \frac{\mu_m - (AE_m + B)}{0.9\mu_{\text{sat}}} \times 100\,\%, \tag{3}$$

where E_m is the exposure for mth point in relative units, μ_{sat} is the saturated signal, A and B are the factors responsible for the slope and shift of the regression line $AE_m + B$. The maximal deviation from linearity for the radiometric curve was 2.7±0.1%.

4.2. Camera dark noise

In this section we present the estimates for the temporal and spatial dark noises for the data processed by the linearising dcraw-converter. For this purpose we detected 64 dark frames at the sensitivity ISO 100 and the exposure time of 1/32 s.

4.2.1. Temporal dark noise

For estimating the temporal component of dark noise we used only the central domain of the dark frames (64×64 pixels). The signals from pixels of this array were averaged over frames and the standard deviation was calculated for each pixel $\sigma_{\text{dt},ij}$. As a result, two arrays were formed: the array of mean values of dark signal A_{ij}^{mean} and the array of standard deviations $\sigma_{\text{dt},ij}$. This procedure follows the method used by PixeLink for estimating dark noise [13]. To quantitatively estimate the temporal dark noise we calculated the mean standard deviation for the array $\sigma_{\text{dt},ij}$

$$N_{\text{dt}} = \sqrt{\frac{1}{kn}\sum_{i,j=1}^{k,n}\sigma_{\text{dt},ij}^2}, \tag{4}$$

where k and n are the numbers of pixels in columns and rows of the dark frame domain used. According to the measurement results, the temporal dark noise is $N_{\text{dt}} \approx 1.6 \pm 0.2$ digital units.

4.2.2. Spatial dark noise

To estimate the spatial dark noise that characterises nonuniformity of the dark signal over pixels we calculated the standard deviation σ_{ds} over the total averaged dark frame. In this case the dark noise is estimated [13] as

$$N_{\text{ds}} = \frac{\sigma_{\text{ds}}}{\mu_{\text{sat}}} \times 100\,\%. \tag{5}$$

For the camera employed we have μ_{sat} = 3470 digital units.

According to the measurement results the mean value of the signal averaged over frame is 256.0±0.4 digital units and the standard deviation is $\sigma_{\text{ds}} \approx 0.4$ digital units. The spatial dark noise is $N_{\text{dss}} \approx 0.01\,\%$. It worth noting that such low spa-

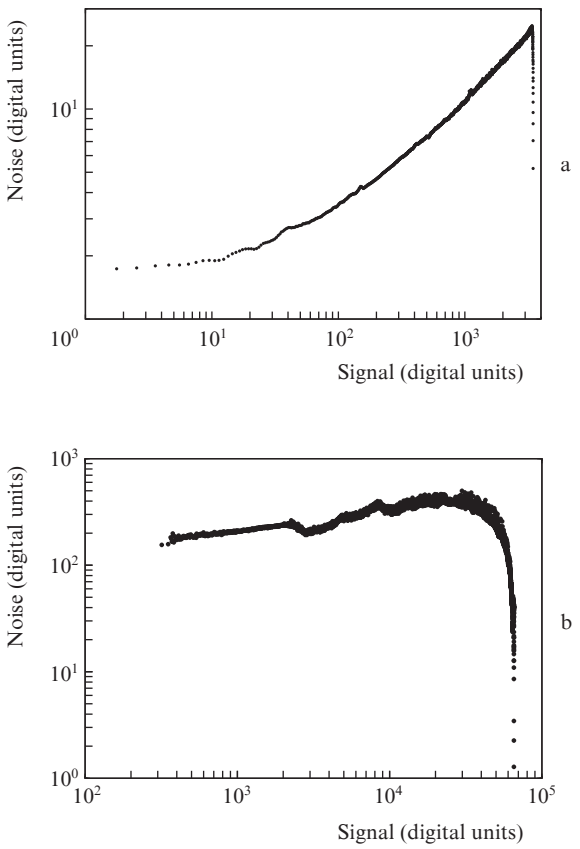

Figure 6. Temporal light noise versus signal amplitude for data processed by dcraw-converter (a) and by authorised converter (b).

tial dark noise is explained by the electronic means of noise suppression in Canon cameras.

4.3. Noises dependent on the light signal value

For the considered digital camera we measured the temporal and spatial (inhomogeneity of photosensitivity) noises dependent on the value of light signal. The measurements were taken separately in each color channel. For measuring in the red channel, odd pixels from odd rows were chosen (row 1, pixels $1, 3, 5, \ldots$; row 3, pixels $1, 3, 5, \ldots$; and so on), in the green channel odd pixels from even rows were chosen (row 1, pixels $2, 4, 6, \ldots$; row 3, pixels $2, 4, 6, \ldots$; and so on), and in the blue channel even pixels from even rows were chosen (row 2, pixels $2, 4, 6, \ldots$; row 2, pixels $2, 4, 6, \ldots$; and so on) according to the Bayer mask. As before, we used the array of white LEDs, whose radiation passed through a diffusing glass for eliminating inhomogeneities of the plane light field. The noise characteristics were estimated from the whole averaged frame.

The measurement results are presented for green color channel only, because the characteristics of color channels are determined by those of the color filters deposited to the array rather than by the characteristics of the device itself (photocells under different color filters are the same). This is confirmed by the fact that the noise characteristics in different color channels coincide within the measurement error.

4.3.1. Temporal light noise

In measuring the parameters of temporal light noise we used a plane source of light radiation with inhomogeneous distribution of brightness over its surface so that the range of illumination of different areas in the image was wider than the dynamic range of the camera under test. We recorded 64 frames of such source. The detected frames were processed by the dcraw-converter in the 'document' regime and, for comparison, by the authorised converter. The images obtained were averaged over frames and became the basis for creating the array of mean signal values in pixels S_{ij}^{mean} and the array of standard deviations $\sigma_{\text{lt},ij}$. Then from array S_{ij}^{mean} the signals were chosen with the step of 1 digital unit. For each signal value from S_{ij}^{mean} the corresponding standard deviation from $\sigma_{\text{lt},ij}$ was found as the estimate of the temporal light noise. The dependence of the temporal light noise on the signal amplitude is shown in Fig. 6a for the dcraw-converter and in Fig. 6b for the authorised camera converter. The noticeable difference between Figs 6a and 6b is explained by the post-processing procedures of images converted by the authorised converter.

The curve on Fig. 6a in linear (non-logarithmical) coordinates is well described by a root function. Hence, the temporal light noise of images processed by the dcraw-converter obeys the Poisson statistics, which describes the photon shot noise. This is an additional confirmation of the linearity of the data obtained from photosensor by using dcraw-converter.

4.3.2. Nonuniformity of the photo response

The measure of the spatial noise dependent on the intensity of detected radiation is the photo response nonuniformity (PRNU). To estimate PRNU we detected and averaged 64 frames of plane light field image. Mean dark signal A_{ij}^{mean} was subtracted from the averaged image (see Section 4.2.1). The obtained averaged image of plane light field was decomposed into three arrays corresponding to the three color channels. Then for each array the standard deviation σ_{ls} and mean light signal (FM) were calculated. Then PRNU for each color component is estimated [13] as follows

$$\text{PRNU} = \frac{\sigma_{\text{ls}}}{\text{FM}} \times 100\%. \tag{6}$$

According to measurement results, at an average light signal of 2300 digital units the average nonuniformity of the photo response over all color channels is $\sim 0.5\%$.

4.4. Estimate of camera dynamic range in detecting light signals

By using the data obtained one can estimate the dynamic range of the digital camera. All estimates are made in the assumption that light is detected with a minimal signal/noise ratio equal to 2 (rather than to conventional value of 1). Such a choice is explained by the fact that the digital camera is of commercial type.

The minimal detectable signal is 4 digital units at the signal/noise ratio equal to 2 (see Fig. 6a). This complies with the estimates obtained for the temporal dark noise (1.6 digital

units) and for spatial dark noise (0.4 digital units). As is seen from Fig. 4a the value of exposure E_{min} corresponding to the minimal detectable signal is 1.3×10^{-3} relative units.

For obtaining the signal value corresponding to the maximum linear dynamic range (3070 digital units, Fig. 4b) the experimental radiometric function was approximated by a linear function; 3070 digital units is the maximal signal, for which the approximating line fits within the measurement error. The exposure for this signal is $E_{max} = 1.0$ relative units. The linear dynamic range D_l estimated from the relationship

$$D_l = 20\lg\frac{E_{max}}{E_{min}} \tag{7}$$

was found to be 58 dB.

For estimating the full dynamic range we determined the saturated signal (3470 digital units), the corresponding exposure is $E_{sat} = 1.12$ relative units (see Fig. 4b). The total dynamic range (D_f) estimated from the relationship

$$D_f = 20\lg\frac{E_{sat}}{E_{min}} \tag{8}$$

is 59 dB.

Similar estimates were made for the data processed by the authorised camera converter. By using the radiometric function obtained (Fig. 3) and taking into account Fig. 6b one can estimate the linear and full dynamic ranges of the camera in detecting nonlinearised data. As above, the minimal signal/noise ratio was taken 2, so the estimated minimal detectable signal was 400 digital units (see Fig. 6b), and the corresponding relative exposure was $E_{min} = 8.2\times10^{-4}$ relative units (Fig. 3a). The maximal value of linear signal resulting from the experimental data approximation (see Fig. 3a) was 24500 digital units. This value corresponds to the utmost experimental value, for which the approximating line fits within the measurement error. The exposure for this signal is $E_{max} = 5.0\times10^{-2}$ relative units (Fig. 3b), and the linear dynamic range is 36 dB (see [7]). Thus, by using a special raw-converter, for example, dcraw one can expand the linear dynamic range of camera by a factor of 10 in detecting light signals.

5. Discussion of results and conclusions

The procedure for extracting linear data from commercial digital photo-cameras is described for measuring spatial distributions of laser radiation intensity. Method is given for estimating the measurement characteristics of such cameras: the linear and total dynamic ranges; temporal and spatial noises, both dark and those depending on the magnitude of detected light signal.

According to the results obtained, in using the procedure for extracting linear data the Canon EOS 400D commercial digital cameras can be employed as the measuring detecting devices with the following characteristics.

(i) The linear dynamic range of camera is 58 dB with the maximal deviation from linearity 2.7%; the full dynamic range is 59 dB. Without using procedures for extracting linear data the linear dynamic range is 36 dB only. Hence, the employment of special dcraw-converter increases the linear dynamic range in detecting light signals by a factor greater than 10.

(ii) Dark temporal noise is 1.6 digital units (the saturated signal for camera is 3470 digital units).

(iii) The measured dependence of temporal noise on the magnitude of detected light signal is similar to the corresponding dependence for technical cameras. This is the confirmation that if the dcraw-converter is used then undesirable post-processing of detected data is absent.

(iv) The spatial dark noise is 0.01% from the maximal signal. This low noise is explained by a noise suppression system based on the correlated double sampling [15] that is used in the sensor.

(v) The photo response nonuniformity (0.5%) is comparable with the corresponding characteristic for technical cameras. This is explained by the electronic noise suppression scheme in the photo-sensor of the Canon EOS 400D camera, which employs the method of complete electronic transfer of charge.

These characteristics of digital commercial camera obtained with the help of linearising dcraw-converter correspond to those of technical measuring cameras. However, there are substantial drawbacks of commercial cameras used for measuring purposes.

(i) Only a part of pixels can be simultaneously used for detecting the intensity distribution of radiation at a particular wavelength (the red and blue color channels use a quarter of all pixels, the green channel uses half the pixels).

(ii) In the general case the dependence of sensor quantum efficiency on radiation wavelength is not known.

(iii) An additional procedure for extracting linear data and separating color channels is needed for obtaining data in measurements.

(iv) The repetition frequency of taking frames cannot be above several frames per second. The synchronising capabilities are limited by software facilities.

Thus, according to the authors, commercial digital cameras may be an inexpensive alternative to technical cameras in detecting intensity spatial distributions of laser sources.

Acknowledgements. The work was performed under the financial support of the Federal Agency on Science and Innovations of the Russian Federation (FANI RF) (State Contract Nos 02.740.11.0433; 02.740.11.0222; P953) and the Russian Foundation for Basic Research (Grant No. 10-02-00399).

References

1. Tucker S.C., Cathey W.Th., Dowski E.R.Jr. *Opt. Express*, **4** (11), 467 (1999).
2. Hamey L.G.C. *Proc. Digital Imaging Computing: Techniques and Applications (DICTA 2005)* (Coirns, Australia, 2005).
3. Plemmons R.J., Horvath M., Leonhardt E., Pauca V.P., Prasad S., Robinson B., Setty H., Torgersen T.C., van der Gracht J., Dowski E., Narayanswamy R., Silveira P.E.X. *Proc. SPIE Int. Soc. Opt. Eng.*, **5559**, 346 (2004).

4. Starikov S.N., Balan N.N., Rodin V.G., Solyakin I.V., Shapkarina E.A. *Proc. SPIE Int. Soc. Opt. Eng.*, **6245**, 62450C (2006).
5. http://www.cybercom.net/~dcoffin/dcraw.
6. Hytti H.T. *Proc. SPIE Int. Soc. Opt. Eng.*, **6059**, 60590A (2005).
7. Starikov S.N., Balan N.N., Konnik M.V., Rodin V.G., Solyakin I.V., Shapkarina E.A., *Proc. SPIE Int. Soc. Opt. Eng.*, **6574**, 65740J (2007).
8. Bayer B.E. US Patent №3,971,065 (1976).
9. Cupitt J., Martinez K. *Proc. SPIE Int. Soc. Opt. Eng.*, **2663**, 19 (1996).
10. Martinez K., Cupitt J. *Proc. Int. Conf. on Image Processing (ICIP 2005)* (Genoa, Italy, 2005) Vol. 2, p.574.
11. Konnik M.V., Starikov S.N., *Proc. SPIE Int. Soc. Opt. Eng.*, **7252**, 72520V (2009).
12. Goodman J.W. *Introduction to Fourier Optics* (New York: McGraw-Hill, 1968).
13. http://www.pixelink.com.
14. http://www.emva.org/standard1288/downloads/emva_standard_1288 _release_a201.
15. Hynecek J. *IEEE Trans. Nucl. Sci.*, **39**, 2497 (1992).